Smeared Fractures: a promising approach to model transfers in fractured media

Andre Fourno, Grenier Christophe, Fred Delay, Emmanuel Mouche, Hakim Benabderrahmane

Smeared Fractures: a promising approach to model transfers in fractured media

A. Fourno[a], C. Grenier[a], F. Delay[b], E. Mouche[a], and H. Benabderrahmane[c]

[a]CEA (Commissariat à l'Énergie Atomique), Centre d'Études de Saclay, 91191 Gif sur Yvette Cedex, France

[b]HYDRASA, Université de Poitiers,
40 Avenue du Recteur Pineau, 86022 Poitiers, France

[c]ANDRA (Agence Nationale pour la Gestion des Déchets Radioactifs), DS/SHG,
Parc de la Croix Blanche, 1-7 rue Jean Monnet, 92298 Châtenay-Malabry, France

In the field of nuclear waste storage, special interest is put on modeling transfer processes in fractured media. It remains a challenging task due to the large contrasts in the properties of different units of the medium, the geometrical complexity of the system and strong level of uncertainties for flow and transport parameters. In addition, modeling approaches should address different times scales: experimental forced flow conditions (several months) and post closure natural flow conditions (thousand of years at least) for which diffusion processes play a major role. To model transfers in fractured media, we developed a smeared fractures approach for a Mixed and Hybrid Finite Element scheme including estimation of associated flow and transport parameters and implemented in our code (CAST3M). This approach is a continuous representation of the fracture block for a regular discretization mesh, the presence of the fracture being taken into account by an heteregeneous field of parameters. The smeared fractures approach, as other continuous approaches, is most appropriate for slow transfers and presents the advantage of taking actual block geometries into account as well as providing good precision results associated to low computer cost. We present here an overview of the evaluation phase for 2D cases. These include results on synthetics and realistic systems, different flow regimes and parameter values. We extend the approach to 3D systems and present preliminary results for flow (3D Äspö -Sweden- geometry, 200m block scale).

1. PRESENTATION OF THE SMEARED FRACTURES APPROACH

The basic idea of the approach is not to mesh the fracture network but to take the presence of fractures into account by means of continuous heterogeneous fields (transmissivity, porosity, head, velocity, concentration...). This line, followed by different authors ([1] and [2]), is referred as Smeared Fracture approach and presents the following advantage: no dedicated spatial discretization effort is required (we use a basic regular mesh, simulations can be done on a rough mesh saving computer time). This makes this kind of approach very promising for taking heterogeneity of properties as well as uncertainties into account within a Monte Carlo framework for instance. Furthermore, the geometry of the matrix blocks where transfers proceed by diffusion is fully taken into account contrary to classical simplified 1D approaches for instance. Nevertheless, continuous heterogeneous field representation of a fractured medium requires a homogenization process at the scale of the mesh considered. From a numerical point of view, constant mesh size as well as constant simulation time step might not be appropriate to simulate contrasted regimes (quick in fracture, slow in matrix).

This approach and preliminary results were previously presented at CMWR2002 [3] and are just briefly summed up here. Initially we work on a regular mesh and we have to identify:
(i) meshes corresponding to a fracture,
(ii) X type cells for which flow entering on one side and exiting through the opposite side,
(iii) Y type cells for which flow exiting through the adjacent side,
(iv) and provide the adapted parameter values (transmissivity, porosity, dispersivity...) to the mesh.
The different stages of the approach are illustrated Figure 1 where we can see the matrix mesh (regular mesh without fracture network mesh), fracture network mesh and the different type of cells. In contrast to other smeared fractures approach, where equivalent transmissivity is established by volume ratios and flow precision is verified in posteriori, we guarantee exact conservation of mass flow for a single fracture.

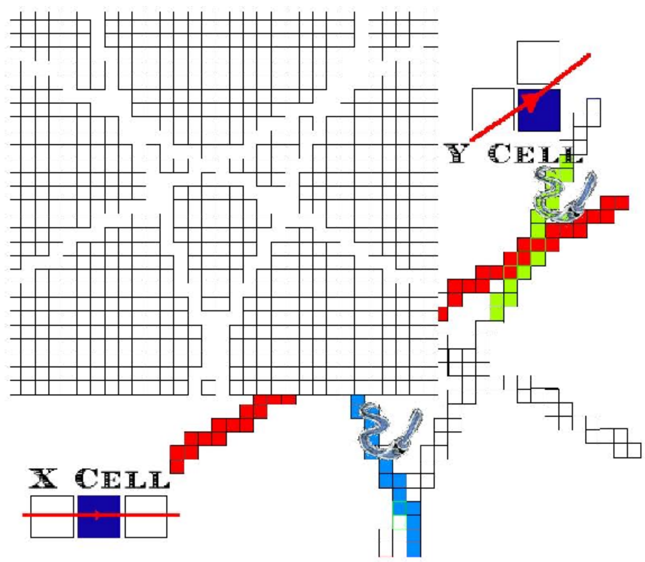

Figure 1. Smeared fractures mesh with X and Y type cells.

- For the flow, the equivalence is based on equality of Darcy flux. The equivalence of the flux through the reference fracture and the equivalent fracture is easy to write

based on the Mixed and Hybrid Finite Element scheme considered. These allow for jointed estimation of the fluxes (gradients) as well as the values of the unknowns within the mesh ([4]). So we can determine a relation between the transmissivity T_{sf} and T_{ref} (sf = smeared fracture and ref = explicit modeling):
$T_{sf} = \frac{(3*N_X+2*N_Y)e}{3*L} * T_{ref}$. where e and L are respectively the aperture and the length of the fracture and N_X and N_Y the number of X and Y type cells. We obtain an exact equivalence for a single fracture.

- For transport, the diffusive flux has the same expression as the Darcy flux. Based on the same considerations as for the equivalent transmissivity (equality of diffusive flux), the equivalent dispersion tensor is here derived as a scalar value $D = \omega D^p + \alpha \|\vec{q}\|$ where ω, D^p, α and $\vec{q}$ are respectively porosity, pore diffusion coefficient, dispersivity and Darcy velocity of the fracture. We can determine a relation between D_{sf} and D_{ref}:
$D_{sf} = \frac{(3N_X+2N_Y)e}{3L} D_{ref}$.
- Equivalent porosity is estimated calculating transition times associated with a Lagrangien approach for both models (smeared fractures and reference). Considering the equality of both times (smeared fractures and reference) we obtain:
$\omega_{sf} = \frac{L*e}{(N_X+N_Y)\Delta^2} \omega_{ref}$

For a fracture network, the same procedure is applied for each conductor, the value affected to an intersection is the maximum of all met in this mesh. The type of transport at the fracture intersections is full mixing.

2. 2D TEST CASES AND APPLICATIONS

The smeared fracture approach has been tested and qualified for permanent flow simulations on different fracture networks (Figure 2) for different flow regimes and parameters values to characterize the limits of the approach. For all of these cases we injected a plume in a cell of the fracture network and imposed head boundary conditions (at the inlets or outlets of fracture or with a head gradient). The flow and transport results are evaluated on test cases involving comparisons with simulation performed on the same system, but the explicit geometry being represented. We first present results for single fracture for which our approach guarantees exact flow and in a second part results for synthetic and realistic systems.

2.1. Single fracture

Matrix diffusion is a key process in the evaluation of the transfer time of a plume in a fractured medium. Matrix zones act as retention zones increasing the transit times. This retention effect is maximal for large matrix diffusion coefficient and for low flow rates (large contact times with the matrix). We study here the sensitivity of the approach to the values of matrix diffusion coefficients. The fracture properties were presented on Table 1.

We choose three matrix pore diffusion coefficients (D_m): $D_1 = 10^{-12}$, $D_2 = 10^{-11}$ and $D_3 = 10^{-10}$ $m^2.s^{-1}$. The plume was injected at 14.3 m of the inlet and we have a unit head difference between the inlet and the outlet of the fracture.

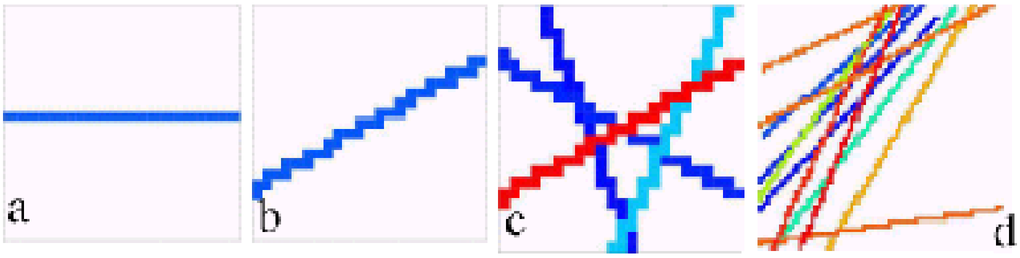

Figure 2. Four test case systems: academic single fracture cases (Figure a and b), 2D synthetic fracture network (Figure c) and 2D realistic system resulting from cut in a block at Äspö (Figure d).

Table 1
Fracture properties and computer cost.

	length m	center	aperture m	transmissivity $m^2.s^{-1}$	porosity
ref. $\Delta_x = 0.4$	57.8	(25. 25.)	0.4	1.10^{-7}	1
sf. $\Delta_x = 0.5$	58.1	(25. 25.)	0.4	$8.22\ 10^{-8}$	0.59

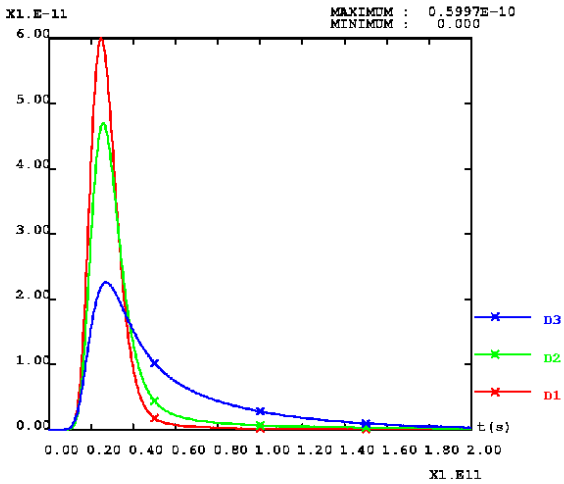

Figure 3. Output mass flux for different D_m (geometry Figure 2b).

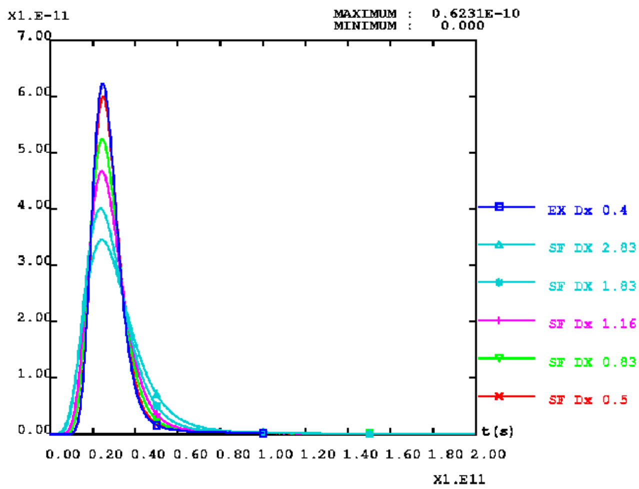

Figure 4. Output mass flux for $D_m = 10^{-12}$ $m^2.s^{-1}$: influence of Δ_x.

The Figures 3 to 6 present results for the three cases. The influence of the matrix diffusion properties shows up classically (refer to [5]) in a little delay in arrival times as well as decrease of the peak level and tailing effects which change the shape of curves

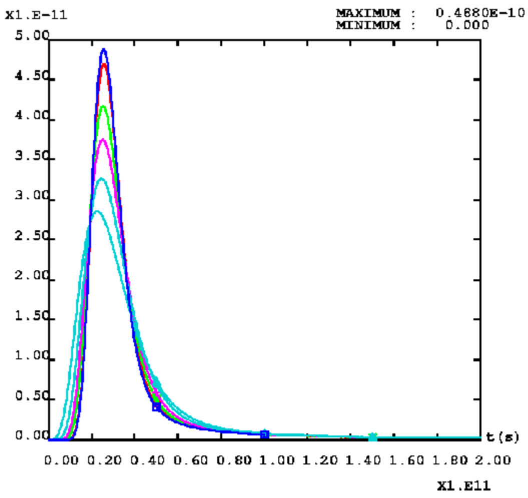

Figure 5. Output mass flux for $D_m = 10^{-11}$ $m^2.s^{-1}$: influence of Δ_x.

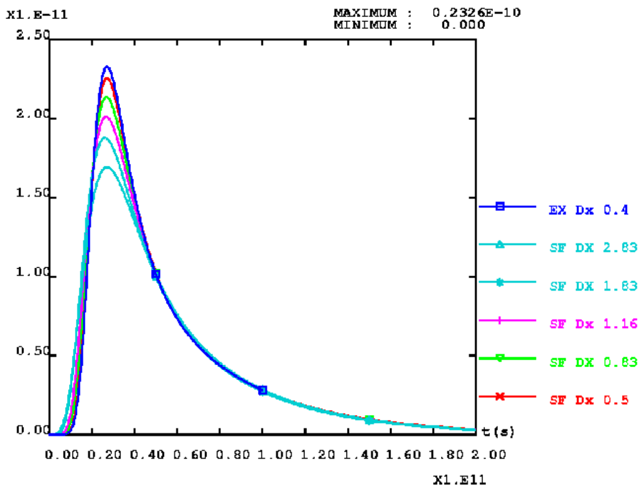

Figure 6. Output mass flux for $D_m = 10^{-10}$ $m^2.s^{-1}$: influence of Δ_x.

(Figure 3). Whatever the discretization and the matrix diffusion coefficient, the error on the peak arrival time between the reference (black curves with squares) and the smeared fractures simulations is weak (a few percent) Figure 3 to 6. For coarse discretization, the smeared fractures approach is more dispersive. Indeed, in these cases, we have a stronger equivalent dispersivity. However, we obtain good precision for the maximal peak value for appropriate discretizations and with low computer cost (Table 2). For a similar discretization ($\Delta_x^{ref} = 0.4$ m and $\Delta_x^{sf} = 0.5$ m), the smeared fracture approach presents a lower computer cost and good precision (Table 2). For the other discretizations, precision depends on role played by matrix diffusion. For dominant diffusive regime, we can choose coarse discretization and obtain satisfactory results (Table 2).

Table 2
Peak level relative error and saved computer cost (single fracture system).

	$\Delta_x^{sf} = 0.5$	$\Delta_x^{sf} = 0.83$	$\Delta_x^{sf} = 1.16$	$\Delta_x^{sf} = 1.83$	$\Delta_x^{sf} = 2.83$
$D_m = 10^{-12}$ error	3%	15%	24%	35%	44%
$D_m = 10^{-11}$ error	3%	14%	23%	33%	41%
$D_m = 10^{-10}$ error	2%	8%	13%	19%	27%
saved computer cost	10%	64%	80%	86%	94%

Results for modeling single fracture show that the finer the grid is, the better the results are. Satisfactory results are easily obtained for low computer cost. The main features of flow and transport are indeed captured by the smeared fracture approach. The next step is to test the approach on fracture networks.

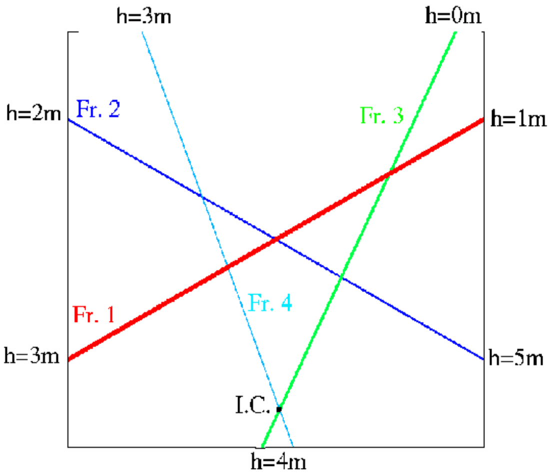

Figure 7. Boundary conditions and initial mass location (I.C.).

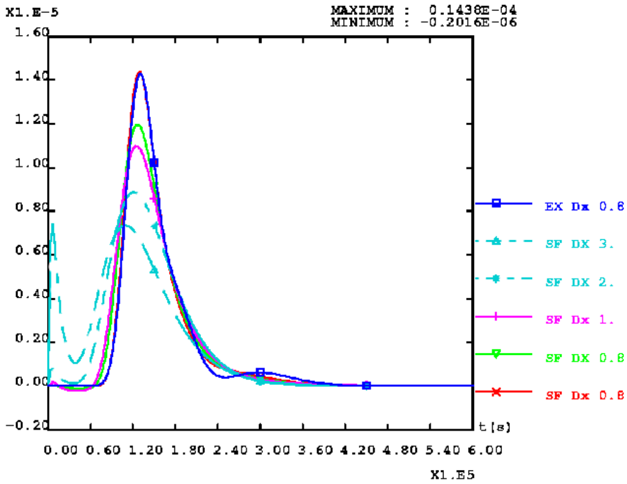

Figure 8. Total fluxes at the outlets for K_1: influence of Δ_x.

2.2. Four synthetic fracture network

This presented fracture system is a synthetic fracture network. The initial transport condition (I.C.) are: unit mass at the fracture 3 and 4 intersection (refer to Figure 7). For each fracture, we choose different boundary conditions for flow problem (Figure 7). We tested this fracture network for three flow regimes (we changed the transmissivity for each fracture):
(i) a dominant advective regime K_1 (matrix diffusion negligible)
(ii) an intermediate regime K_2
(iii) a dominant diffusive regime K_3 (important matrix diffusion)
We present breakthrough curves at the limits of the domains for the three regimes on Figure 8 to 10. The black curves with squares correspond to the reference calculation.

Globally, the smeared fractures approach works better:

1. when refining the mesh
   For each regime, we can see our approach has better precision for finest mesh (Table 3).

2. for dominant diffusive regimes
   We can see in Table 3 that the more the role played by the matrix is important the better is the precision. It can easily be explain. When we model a fracture system we have to take two criterions into account :
   - $(Nc = \frac{q*\Delta t}{\omega*\Delta x}) < 1$ in the fracture
   - $(F_0^x = \frac{2*D_{ii}*\Delta t}{\omega*\Delta x^2}) > \frac{1}{6}$ in the matrix, where Δ_t is the time discretization.
   With the smeared fracture approach we work with a regular mesh. For advective regime, matrix blocks in the smeared fractures approach are potentially under-discretized (we do not respect the second criterion). For dominant diffusive regime, retardation due to matrix diffusion is large so that contrasts in fracture and matrix

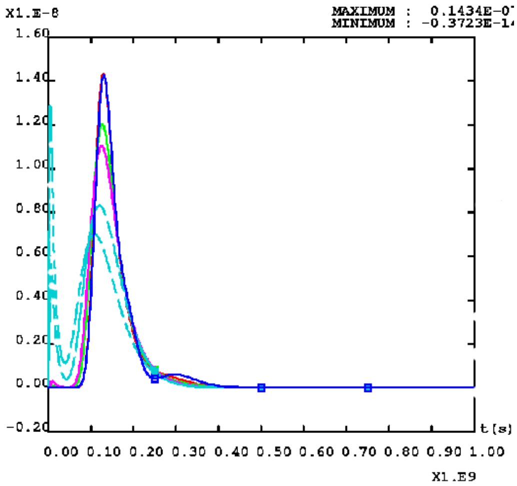

Figure 9. Total fluxes at the outlets for K_2: influence of Δ_x.

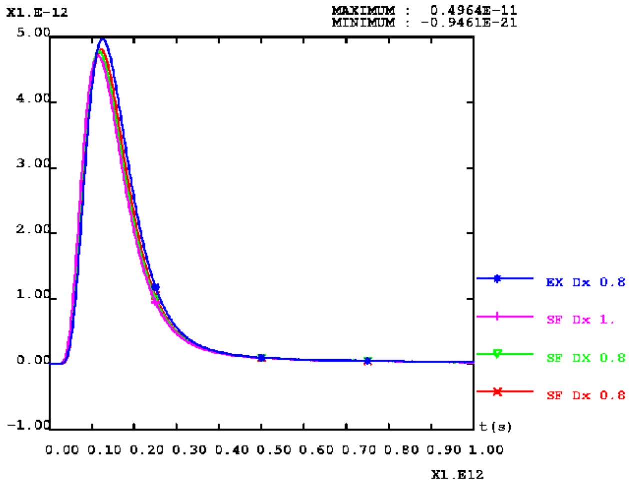

Figure 10. Total fluxes at the outlets for K_3: influence of Δ_x.

are weaker. It's easier to satisfy these criterions. That is why the smeared fracture approach results are better for long time scale simulations (Table 3) for which we can use coarse discretization. Finely this approach is very interesting for long time scale and post closure simulations.

Table 3
Peak level relative error and saved computer cost (4 fracture system).

	$\Delta X = 0.5$	$\Delta X = 0.8$	$\Delta X = 1.$
K_1 error	0%	16%	23%
K_2 error	0%	15%	21%
K_3 error	3%	4%	5%
saved computer cost	30%	60%	70%

Nevertheless limits of the approach appears.
- For coarse mesh, we obtain bad results, if we loose the fracture geometry (for coarse mesh matrix zones can be lost) (dotted curves Figures 8 and 9).
- We can observe that the smeared fracture approach smooths the breakthrough curves; we don't see as well as the reference curve, the impact of each fracture (second peak disappear in the smeared fractures curves Figure 8 and 9).
If we pay attention to these limits, the approach stays promising. Dominant diffusive regime modeling can be done with coarse discretization with the smeared fractures approach and provide good results with low computer cost. For other regimes we have to

use finest discretization to obtain results with good precision (Table 3). Now we can test the approach on realistic systems.

2.3. 2D system from a block at Äspö.

The 2D Äspö case results from a cut in the actual 3D geometry (200m block scale). For more information about Äspö, refer to [6]. The initial transport condition (I.C.) are: unit mass in an intersection (Figure 11). We take a head gradient of 10^{-3} in agreement with local natural flow conditions (from top right to bottom left on Figure 11).

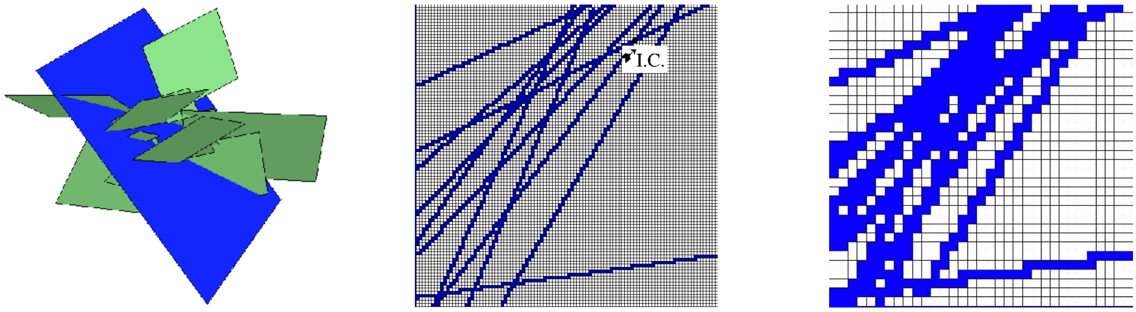

Figure 11. 3D Äspö fractured site at 200m scale and smeared fracture mesh (high and low levels of discretization.

We study the influence of matrix diffusion:

- In a first step we modeled the system without the matrix diffusion. The breakthrough curves at the limits of the system have several peaks. These peak correspond to different paths followed by the plume. For each peak, we are able to determine its paths (Figure 12).
- In a second step we take matrix diffusion (matrix pore diffusion coefficient $D_e = 10^{-11}\ m^2.s^{-1}$) into account and compare breakthrough curves. The role played by the matrix diffusion shows up by an arrival time delays, a decrease of peak value and a tail (Figure 13). But we have an other effect: where we have five peaks for the no matrix diffusion case we have just three peaks when we consider the matrix diffusion. In fact, when the plume can diffuse in the matrix, the peaks decrease and the breakthrough curves spread out. Diffusion into the matrix zones has a smoothing effect (refer to Figure 13).

Our smeared fractures approach provides good results with low computer cost:
- The peak arrival times are in agreement with the reference case.
- The peak value are an average of different peak levels (dispersivity effect).
- When the diffusion effect smooth the breakthrough curves, smeared fractures approach provides better results (peak level contrasts are weaker and so their averages are close to their values).
For this fracture system, we can't test the effect of under-discretization because for coarse

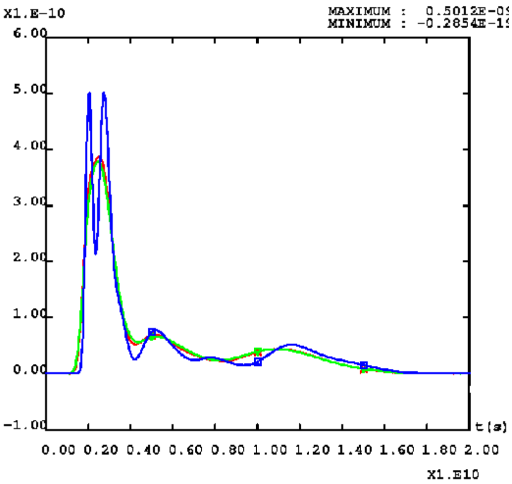

Figure 12. Breakthrough curves without matrix diffusion.

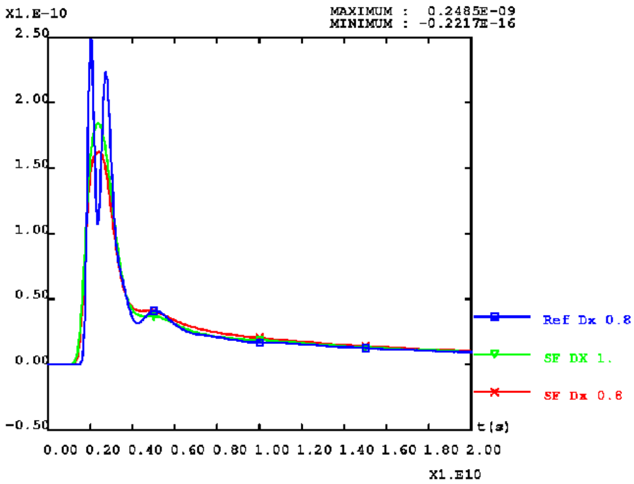

Figure 13. Breakthrough curves with matrix diffusion.

discretizations, we loose geometry of the fracture network as shown on Figure 11 low level of discretization.

2.4. Modeling conclusions for 2D

This approach provides good results in terms of precision, low computer cost. The quality of the results depends on the importance of the matrix diffusion as well as mesh size. The smeared fractures approach is more specially dedicated to long transport time as for post closure conditions where the actual geometry of the matrix blocks can be taken into account.

3. 3D PRELIMINARY RESULTS

Extension to 3D cases is not directly possible. For a 3D single fracture, we first determine equivalent tensorial properties depending on regular mesh direction and fracture slope. As we want to represent the equivalent properties by scalars, we study the variation of equivalent tensorial properties for different fracture slopes and different head gradient orientation. If we consider a 3D single fracture modeled with the smeared fracture approach and with the equivalent permeability $K_{sf} = C * K_{ref}$ where C is a correcting coefficient, we proved C is bounded whatever the fracture slope and the head gradient bearings. We have:
$\frac{e}{2\Delta_x} < C < \frac{4e}{3\Delta_x}$.
We choose to use $C = \frac{e}{\Delta_x}$ to minimize the absolute error. We applied the approach on the 3D Äspö fractured site at 200m scale. Figure 14 presents the smeared fracture mesh used and the fracture permeability.

We use the head boundary data of the Äspö site and model a pumping test correspondint on tracer test C2 of Äspö task 6 (refer to [6]). The pumping location is in the center of the

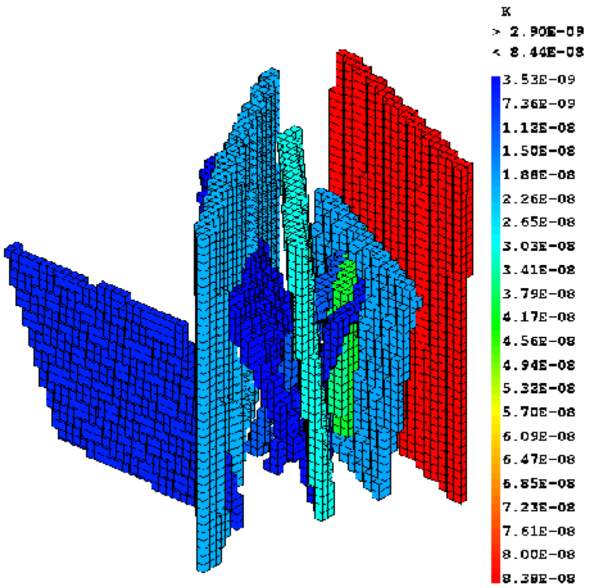

Figure 14. Fracture network equivalent permeability $(m.s^{-1})$.

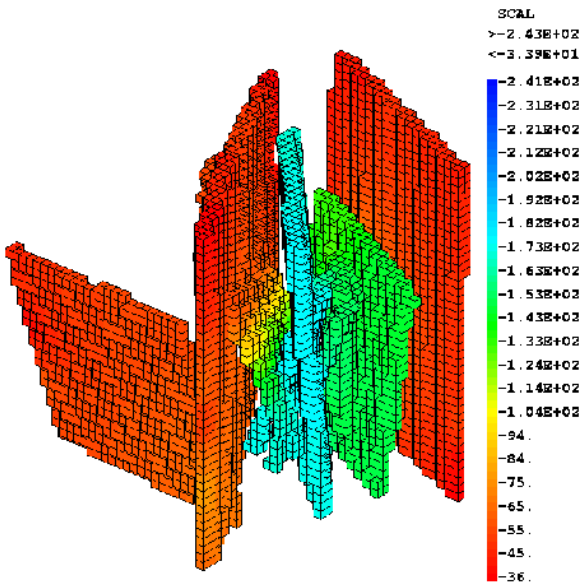

Figure 15. Head Field (m).

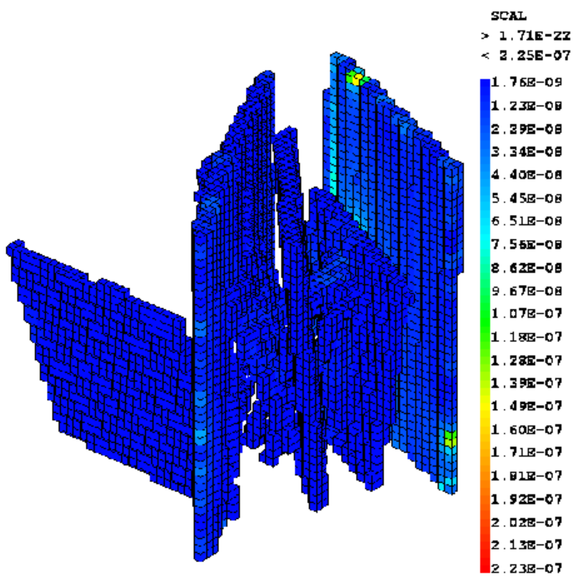

Figure 16. Darcy velocity $(m.s^{-1})$.

fracture network and we have a pumping rate of $3.25.10^{-5}$ $m^3.s^{-1}$. Results are presented on Figure 15 and 16.

These results were obtained for low computer cost. Nevertheless ongoing work is required to establish their precision.

4. CONCLUSIONS AND PERSPECTIVES

For 2D modeling, this approach provides good results in terms of precision, low computer cost. The quality of results more closely depends on the importance of the matrix diffusion as well as mesh size. It appears that this approach is more dedicated to long time scale as for post closure conditions where matrix diffusion is important. For the 3D modeling, preliminary results are presented but more work is required to asses their quality.

REFERENCES

1. U. Svensson. A continuum representation of fracture networks. Part I : Method and basic test cases. Journal of Hydrology 250, pp. 170-186, 2001.
2. Y. Tanaka, K. Minyakawa, T. Igarashi, Y. Shigeno. Application of 3D smeared fracture model to the hydraulic impact of the Äspö tunnel. SKB Report. ICR 96-07, 1996.
3. A. Fourno, C. Grenier, E. Mouche, G. Thouvenin and H. Benabderahmane. Qualification and validity of a smeared fractures modelling approach for flow and transport in fractured media. Computational Methods in Water Resources. Volume 1, pp. 319-326, 2002.
4. F. Dabbene. Mixed Hybrid Finite Elements for transport of pollutants by underground water. Proc. 10th conference on finite elements in fluids, Tucson, Arizona, 1998.
5. Neretnieks. Diffusion in the rock matrix: an importantfactor in radionuclide retardation ? Journal of Geophysical Research, Vol. 85, No B8, 1980.
6. ÄSPÖ-TF web site for the ÄSPÖ Task Force under http://www.skb.se/taskforce.